Applied Physics Letters

Buckling of metallic glass supercooled liquid layer during embossing

Cite as: Appl. Phys. Lett. **114**, 113102 (2019); https://doi.org/10.1063/1.5091721
Submitted: 05 February 2019 . Accepted: 26 February 2019 . Published Online: 19 March 2019

Chandra Sekhar Meduri, Zhonglue Hu, Jerzy Blawzdziewicz, and Golden Kumar

Applied Physics Letters ARTICLE scitation.org/journal/apl

Buckling of metallic glass supercooled liquid layer during embossing

Cite as: Appl. Phys. Lett. **114**, 113102 (2019); doi: 10.1063/1.5091721
Submitted: 5 February 2019 · Accepted: 26 February 2019 ·
Published Online: 19 March 2019

Chandra Sekhar Meduri,[1] Zhonglue Hu,[1] Jerzy Blawzdziewicz,[1] and Golden Kumar[2,a)]

AFFILIATIONS

[1]Department of Mechanical Engineering, Texas Tech University, Lubbock, Texas 79409, USA
[2]Department of Mechanical Engineering, The University of Texas at Dallas, Richardson, Texas 75080, USA

[a)]Author to whom correspondence should be addressed: Golden.Kumar@UTDallas.edu

ABSTRACT

Embossing of metallic glass supercooled liquids into templates is emerging as a precision net-shaping and surface patterning technique for metals. Here, we report the effect of thickness of metallic glass on template-based embossing. The results show that the existing embossing theory developed for thick samples fails to describe the process when the thickness of metallic glass becomes comparable to the template cavity diameter. The increased flow resistance at the cavity entrance results in viscous buckling of supercooled liquid instead of filling. A phenomenological equation is proposed to describe the thickness dependent filling of template cavities. The buckling phenomenon is analyzed based on the folding model of multilayer viscous media. We show that controlled buckling can be harnessed in the fabrication of metal microtubes, which are desirable for many emerging applications.

The supercooled liquid state of metallic glasses has been utilized in a wide range of thermoplastic forming operations such as embossing,[1–3] blow molding,[4,5] extrusion,[6] rolling,[7,8] and drawing.[9,10] Parallel-plate embossing has gained increasing attention due to its ability to produce nanoscale structures using simple hardware.[11,12] In embossing, a sheet of metallic glass is pressed onto a rigid template using two parallel plates heated above the glass transition temperature (T_g) of the metallic glass.[1,2,13] Above T_g, the metallic glass becomes a metastable supercooled liquid which can fill the template features under pressure. Thermoplastic embossing of metallic glasses is typically carried out in air using standard compression testing machines equipped with heating provision.[1,2,13] The technique has been used to fabricate precise 3D microparts,[1] controllable nanostructures,[14] and hierarchically textured surfaces[9] from various metallic glass formers.

The filling of template cavities during embossing has been described by assuming the Newtonian behavior of metallic glass supercooled liquids and creeping flow conditions.[1,15–18] The earlier studies proposed a modified Hagen-Poiseuille equation[1] to predict the template filling as a function of embossing parameters and supercooled liquid properties. Neglecting the capillary pressure and the oxidation related terms, the embossing pressure for a cylindrical cavity can be expressed as

$$P \approx \frac{32\eta}{t}\left(\frac{L}{D}\right)^2, \tag{1}$$

where P is the embossing pressure at the entrance of the cavity, L is the filling length, D is the cavity diameter, η is the viscosity of supercooled liquid, and t is the embossing time. The pressure dependence on L (or L/D ratio) suggests that the viscous resistance at the cavity entrance was neglected (i.e., the infinite supply of metallic glass was assumed), and only the flow resistance along the length of the cavity was considered. The equation yielded good agreement because the typical thicknesses (>500 μm) of metallic glass used in experiments are larger than the lithographic template features ($D < 100$ μm). However, as we demonstrate in this study, Eq. (1) does not accurately describe the template filling when the thickness of metallic glass becomes comparable or smaller than the cavity diameter. Figure 1 shows an example of $Pt_{57.5}Cu_{14.7}Ni_{5.3}P_{22.5}$ (Pt-based) metallic glass of varying initial thicknesses (2.5D, D, and 0.25D) thermoplastically embossed onto a cylindrical cavity under the same conditions. The filling length is in good agreement with Eq. (1) for the thick sample (2.5D) but deviates significantly for the thin samples (D and 0.25D). In addition, the thinner specimens show the formation of buckles as visualized in the images of the top surfaces [Figs. 1(b) and 1(c)]. Buckles are not observed [Fig. 1(a)] when the metallic glass thickness was greater than the cavity diameter. Similar effects have been observed in thermoplastic embossing of thin polymer films.[19–21] With increasing interest in metallic glass thin films,[22–24] it is important to investigate the effect of thickness on embossing. In addition, controlled buckling can lead to

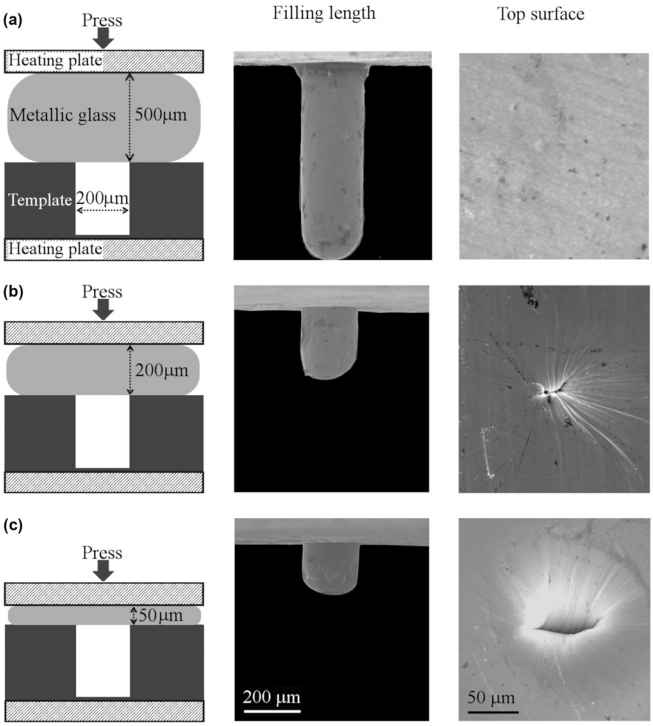

FIG. 1. Thermoplastic embossing of Pt-based metallic glass with varying thicknesses against a cylindrical cavity of diameter 200 μm. The scanning electron microscopy (SEM) images of the embossed pillars and the top surfaces show significant effects of thickness on the embossing process. The filling length is shorter in thin samples, and the corresponding top surfaces show the formation of wrinkles and hollow indents. The surface instabilities form when the thickness approaches the cavity diameter during embossing.

interesting applications in micro/nanofabrication.[25,26] The present work is aimed to understand the effect of metallic glass thickness on the filling length (L) and buckle formation during thermoplastic embossing. Pt-based metallic glass is used as a model material because of its oxidation resistance and superior thermoplastic formability.[1,9,16] The details about the synthesis of Pt-based metallic glass have been reported elsewhere.[1]

A schematic of the cross-sectional view of thermoplastic embossing used in the present study is shown in Fig. 2. A disk of metallic glass with the initial radius (R_i) and thickness (H_i) is placed on a cylindrical cavity machined in aluminum (Al). The setup is heated above the glass transition temperature (T_g) of the metallic glass using two parallel heating plates. A time-varying load $F = \beta t$ is applied (where β is the loading rate and t is the embossing time). The accumulated load (Q) is the area under the load-time curve which determines the extent of thermoplastic deformation of metallic glass.[16] The metallic glass flows vertically into the template cavity and laterally due to unrestrained geometry. As a result, the thickness (H) of the residual metallic glass layer decreases, while the radius (R) and filling length (L) increase during embossing.

The viscosity of metallic glass supercooled liquids is of the order of 10^5–10^9 Pa s.[15] Hence, the previous investigations have used Stokes flow equations to describe the disk flattening and cavity filling process

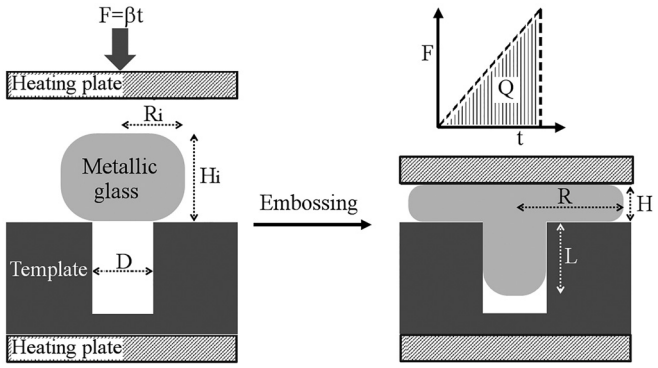

FIG. 2. Illustration of the experimental procedure used to study the effects of metallic glass thickness, template cavity diameter, and loading on embossing. The metallic glass of varying initial thicknesses is embossed under linearly increasing load (F). The load, the loading rate, and the cavity diameter (D) are varied, but the processing temperature is kept constant. The accumulated load (Q) is the area under the load-time curve.

during embossing.[16,27] As explained in the supplementary material, a simple scaling analysis relating the viscous resistance contributions at the cavity entrance and applied pressure can be formulated as

$$P \approx \left[\frac{16\eta L}{D^2}\right]\frac{dL}{dt} + \left[\frac{\pi\mu\eta D^2}{H^3}\right]\frac{dL}{dt}, \tag{2}$$

where μ is the lateral flow resistance coefficient and was used as a fitting parameter to match the experimental results (Fig. 3). The first term in Eq. (2) corresponds to the flow resistance along the cavity length, and the second term corresponds to the lateral flow resistance (acting along the radius of the metallic glass disk). At large H (or the H/D ratio) values, the second term becomes negligible, and the equation reduces to Eq. (1). The second term becomes significant and starts to influence the filling process (Figs. 1 and 3) when H becomes comparable or smaller than D. For convenience of integration, we consider H a time invariant (valid for samples with a small thickness variation during embossing) and obtain the solution for Eq. (2) as

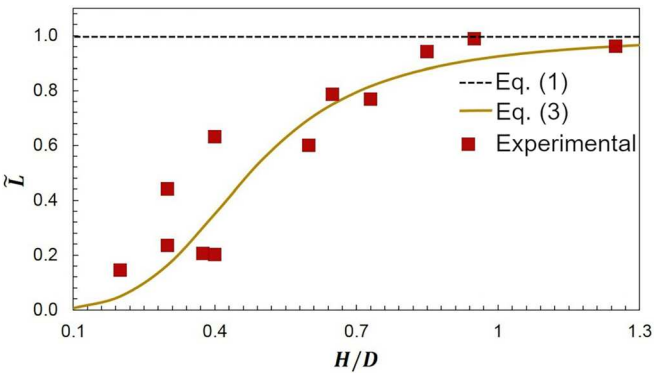

FIG. 3. Effect of metallic glass thickness on the normalized filling length ($\bar{L}$). The comparison of the measured values (red squares), the existing theory [Eq. (1)], and the proposed model [Eq. (3)] is shown.

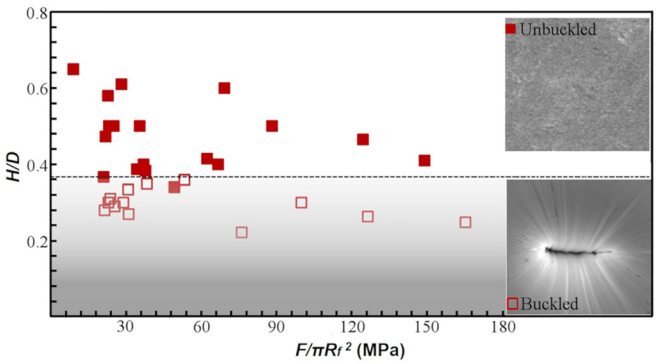

FIG. 4. Normalized final thickness (*H*/*D*) as a function of maximum applied pressure. The buckled and unbuckled samples are labeled based on the SEM images like the ones shown in insets. The buckling is observed the below critical *H*/*D* ratio irrespective of the embossing pressure. Here, Rf is the final disk radius.

$$\tilde{L} = -\alpha\left[\frac{H}{D}\right]^{-3} + \left[\alpha^2\left[\frac{H}{D}\right]^{-6} + 1\right]^{1/2}, \quad (3)$$

where $\tilde{L}$ is the non-dimensional reduced filling length [Eq. (8) in the supplementary material] and α is a non-dimensional parameter related to lateral flow resistance μ in Eq. (2). $\tilde{L}$ is the L/D ratio obtained by solving Eq. (2) and normalized by the maximum L/D attainable for the given loading conditions. The maximum L/D is calculated from Eq. (1). Equation (3) can be used for any thickness, while Eq. (1) is the upper bound and valid only for thick samples. Figure 3 compares the experimental and calculated $\tilde{L}$ [Eq. (3)] values for varying H/D ratios. The experimental values match well with the theoretical calculations, and Eq. (3) captures the observed thickness dependence on the filling length. The H values on the abscissa correspond to the thickness of the metallic glass measured after embossing. At all H/D values greater than 1, the observed filling length approaches the maximum filling length (i.e., $\tilde{L} = 1$). However, for $H/D < 1$, $\tilde{L}$ decreases with decreasing H/D, indicating lesser filling for thin samples. The observed scatter in the measured $\tilde{L}$ at small H/D values is due to the machine compliance, which affects the actual area of contact between the heated plates and the metallic glass disk, and thus the applied pressure.

Another interesting effect of thickness is the buckling of metallic glass supercooled liquid. As shown in Fig. 1, the thin metallic glass buckles/folds into the template cavity, while the thick sample does not show such instability. Although the observed thickness (geometric parameter) dependence of buckling hints towards its viscous nature, it is important to verify the absence or presence of an elastic contribution. A series of embossing experiments were performed by varying the initial thickness, load, and embossing time. A viscous buckling should only depend on the geometric factor, while an elastic buckling requires a critical stress. Figure 4 shows a plot between the non-dimensional final thickness (H/D) and load (F) normalized by the final disk area. The two sets of data points correspond to buckled (open squares) and unbuckled (filled squares) samples. As shown in the insets, the samples with no surface deformation were labeled as unbuckled, while any observable surface feature was considered as an indication of buckling. It is evident from Fig. 4 that (i) the unbuckled-to-buckled transition occurs at a critical H/D value in the range of ~0.36–0.4 (i.e., geometric parameters govern the buckle formation) and (ii) the critical H/D value is independent of the applied load/pressure (i.e., there is no threshold stress for the initiation of buckling). These observations suggest that the observed buckling is viscous in nature, and elastic effects can be ruled out.

The embossing experiments always resulted in some amount of cavity filling prior to buckling. This can be envisioned as buckling of the viscous metallic glass layer embedded between a rigid plate and a viscous metallic glass column as schematically shown in Fig. 5(a). The thin metallic glass layer is subjected to in-plane compression due to high lateral flow resistance. The buckling of thin viscous and elastic multilayers has been studied in geological[28–31] and self-assembly[26,32] systems. The buckling wavelength (λ) can be predicted from the layer thickness and the ratios of viscosity (or elastic constant) values.[29,30] In the current system, the presence of the template cavity confines the maximum wavelength to 2D. The critical thickness corresponding to this buckling wavelength can be estimated as $\sim\lambda/4$ (=0.5D) from the model developed by Biot[29] and Ramberg[33] Despite different geometries in theoretical models, the calculated thickness (0.5D) for buckling is reasonably close to the observed value of 0.4D. Although buckling is undesirable in template imprinting, we show that it can be harnessed in the fabrication of metal microtubes [Fig. 5(b)]. The metallic glass and the template are pulled apart after the formation of a buckle on the top of the solid pillar. The buckle gets elongated, resulting in the formation of a hollow metallic structure, which is subsequently cooled and fractured at room temperature. Figure 5(b) shows an SEM image of the representative sample fabricated using this procedure. The proposed methodology can be applied to multiple buckles to make an array of metallic microtubes, which otherwise require complex processing steps.[34] The opening of microtubes can be controlled by tuning the buckle size. Metal microtubes are desired for applications in transdermal drug-delivery,[35] microfluidics,[36] and sensing.[37]

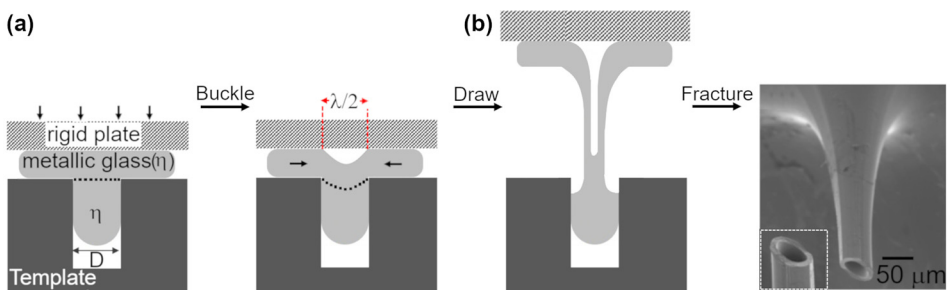

FIG. 5. (a) Schematic of the cross-sectional view of buckle formation with a wavelength (λ). (b) Fabrication of the hollow metallic structure by elongation of the buckle. The SEM image of the Pt-based metallic glass microtube produced by buckling and elongation is shown.

In summary, we have demonstrated that the template-based thermoplastic embossing of metallic glasses is sensitive to their thickness. A general flow model for all thicknesses is developed, whereas the earlier models are valid only for embossing of thick metallic glasses. Significant reduction in the filling length is observed when the metallic glass thickness becomes comparable or smaller than the diameter of template cavities. In this regime, the supercooled liquid undergoes buckling due to mounting lateral flow resistance. The buckling wavelength can be predicted based on the existing theories for viscous buckling of multilayer systems. We further show that the thickness dependent buckling of metallic glass can be utilized in manufacturing of hollow metal structures whose applications will be explored in our future work.

See supplementary material for the derivation of equations for cavity filling and disk thinning during thermoplastic embossing of metallic glass.

This work was supported by the National Science Foundation (NSF) through Award No. CMMI-1663568 and CAREER Award No. CMMI-1653938. J.B. was partially supported by NSF Award No. CBET-1603627. Microscopy characterization was performed using a Hitachi S-4300 SEM acquired through the NSF Major Research Instrumentation Program Award No. #0421032.

REFERENCES

[1]G. Kumar, H. X. Tang, and J. Schroers, Nature **457**, 868 (2009).
[2]M. Hasan, J. Schroers, and G. Kumar, Nano Lett. **15**, 963 (2015).
[3]T. Xia, N. Li, Y. Wu, and L. Liu, Appl. Phys. Lett. **101**, 081601 (2012).
[4]B. Sarac, G. Kumar, T. Hodges, S. Ding, A. Desai, and J. Schroers, J. Microelectromech. Syst. **20**, 28 (2011).
[5]J. Schroers, T. M. Hodges, G. Kumar, H. Raman, A. J. Barnes, and T. A. Waniuk, Mater. Today **14**, 14 (2011).
[6]Y. Kawamura, T. Shibata, A. Inoue, and T. Masumoto, Acta Mater. **46**, 253 (1998).
[7]R. Martinez, G. Kumar, and J. Schroers, Scr. Mater. **59**, 187 (2008).
[8]X. Xiao, S. S. Fang, Q. Wang, G. M. Wang, Q. Hua, and Y. D. Dong, Mater. Lett. **58**, 2357 (2004).
[9]M. Hasan and G. Kumar, Nanoscale **9**, 3261 (2017).
[10]Z. Hu, C. S. Meduri, J. Blawzdziewicz, and G. Kumar, Nanotechnology **30**, 075302 (2019).
[11]G. Kumar, A. Desai, and J. Schroers, Adv. Mater. **23**, 461 (2011).
[12]L. Liu, M. Hasan, and G. Kumar, Nanoscale **6**, 2027 (2014).
[13]Z. Hu, S. Gorumlu, B. Aksak, and G. Kumar, Scr. Mater. **108**, 15 (2015).
[14]C. Uzun, C. Meduri, N. Kahler, L. G. de Peralta, J. M. McCollum, M. Pantoya, G. Kumar, and A. A. Bernussi, J. Appl. Phys. **125**, 015102 (2019).
[15]Y. Kawamura, T. Nakamura, H. Kato, H. Mano, and A. Inoue, Mater. Sci. Eng. A **304–306**, 674 (2001).
[16]G. Kumar, J. Blawzdziewicz, and J. Schroers, Nanotechnology **24**, 105301 (2013).
[17]J. Lu, G. Ravichandran, and W. L. Johnson, Acta Mater. **51**, 3429 (2003).
[18]A. Reger-Leonhard, M. Heilmaier, and J. Eckert, Scr. Mater. **43**, 459 (2000).
[19]C. H. Lin and R. S. Chen, J. Micromech. Microeng. **17**, 1220 (2007).
[20]H. D. Rowland, A. C. Sun, P. R. Schunk, and W. P. King, J. Micromech. Microeng. **15**, 2414 (2005).
[21]Y. Xu, F. Tsumori, T. Toyooka, H. Kotera, and H. Miura, Jpn. J. Appl. Phys. Part 1 **50**, 06GK11 (2011).
[22]M. Ghidelli, H. Idrissi, S. Gravier, J. J. Blandin, J. P. Raskin, D. Schryvers, and T. Pardoen, Acta Mater. **131**, 246 (2017).
[23]C. W. Wang, P. Yiu, J. P. Chu, C. H. Shek, and C. H. Hsueh, J. Mater. Sci. **50**, 2085 (2015).
[24]Y. Liu, J. Padmanabhan, B. Cheung, J. Liu, Z. Chen, B. E. Scanley, D. Wesolowski, M. Pressley, C. C. Broadbridge, S. Altman, and U. D. Schwarz, Sci. Rep. **6**, 26950 (2016).
[25]D. C. Hyun, G. D. Moon, C. J. Park, B. S. Kim, Y. Xia, and U. Jeong, Adv. Mater. **22**, 2642 (2010).
[26]P. J. Yoo, K. Y. Suh, S. Y. Park, and H. H. Lee, Adv. Mater. **14**, 1383 (2002).
[27]N. Li, W. Chen, and L. Liu, JOM **68**, 1246 (2016).
[28]M. A. Biot, Proc. R. Soc. London A: Math. Phys. Sci. **242**, 444 (1957).
[29]M. A. Biot, Geol. Soc. Am. Bull. **72**, 1595 (1961).
[30]M. A. Biot, H. Ode, and W. L. Roever, Geol. Soc. Am. Bull. **72**, 1621 (1961).
[31]J. H. Fink and R. C. Fletcher, J. Volcanol. Geotherm. Res. **4**, 151 (1978).
[32]A. Schweikart, A. Horn, A. Böker, and A. Fery, Complex Macromol. Syst. I **227**, 75 (2010).
[33]H. Ramberg, AAPG Bull. **47**, 484 (1963), https://pubs.geoscienceworld.org/aapgbull/article-abstract/47/3/484/34987/fluid-dynamics-of-viscous-buckling-applicable-to?redirectedFrom=fulltext.
[34]Z. L. Xiang, J. Q. Liu, and C. Lee, Microsyst. Nanoeng. **2**, 16012 (2016).
[35]H. J. Gardeniers, R. Luttge, E. J. Berenschot, M. J. De Boer, S. Y. Yeshurun, M. Hefetz, R. van't Oever, and A. van den Berg, J. Microelectromech. Syst. **12**, 855 (2003).
[36]D. J. Thurmer, C. Deneke, Y. Mei, and O. G. Schmidt, Appl. Phys. Lett. **89**, 223507 (2006).
[37]T. Kipp, H. Welsch, C. Strelow, C. Heyn, and D. Heitmann, Phys. Rev. Lett. **96**, 077403 (2006).